

Giulia Bampa¹, Winfried Leidemann^{1,2}, and Hartmuth Arenhövel³¹*Dipartimento di Fisica, Università di Trento, I-38100 Trento, Italy*²*Istituto Nazionale di Fisica Nucleare, Gruppo Collegato di Trento, Italy*³*Institut für Kernphysik, Johannes Gutenberg-Universität, D-55099 Mainz, Germany*

(Dated: November 6, 2018)

The application of the Lorentz integral transform (LIT) method to photon scattering off nuclei is presented in general. As an example, elastic photon scattering off the deuteron in the unretarded dipole approximation is considered using the LIT method. The inversion of the integral transform is discussed in detail paying particular attention to the high-energy contributions in the resonance term. The obtained E1-polarizabilities are compared to results from the literature. The corresponding theoretical cross section is confronted with experimental results confirming, as already known from previous studies, that the E1-contribution is the most important one at lower energies.

PACS numbers: 21.45.-v, 21.45.Bc, 25.20.Dc

I. INTRODUCTION

The study of electromagnetic reactions in photoabsorption and photon scattering on nuclei is an excellent tool to investigate nuclear structure. In addition, it can also lead to valuable insights into the properties of the nuclear constituents, the nucleons, like for example, electric and magnetic polarizabilities. In this context photon scattering experiments are a particularly interesting source of information on off-shell properties. On the other hand genuine microscopic calculations of photon scattering cross sections are rather complicated since the complete nuclear excitation spectrum has to be taken into account. Thus it hardly comes as a surprise that in the past such theoretical efforts were mainly concentrated on the two-nucleon system. A first realistic calculation of deuteron photon scattering has been carried out in [1]. In the last decade quite a few theoretical investigations have been performed [2–6] among them also calculations based on chiral effective field theory.

Considering a more complex A -nucleon system, as mentioned, one needs to have under control the corresponding A -body continuum. Today this could in principle be realized for the three-nucleon system, but many-body calculations of photon scattering cross sections for systems with $A > 3$ are presently out of reach. On the other hand, there is a particular interest in ${}^6\text{Li}$ photon scattering recently, and data have already been taken at HIGS [7]. Fortunately, the problem of calculating the correct many-body continuum wave function can be avoided by application of the Lorentz integral transform (LIT) method [8, 9]. In fact, the LIT approach reduces a scattering state problem to a simpler bound-state like problem, which then can be solved with techniques that usually are applied for bound states. This leads to an enormous reduction of the complexity of the calculation, e.g., LIT calculations of the total photoabsorption cross sections have even been made for the six- and seven-body nuclei taking into account all possible break-up channels and with full consideration of the final state interaction [10, 11]. In view of the fact, that till now the LIT method has not been applied to photon scattering, we want to demonstrate with the present work the usefulness of this method for this process choosing as a test case the deuteron. That has the advantage that first of all, the calculation is quite simple and furthermore allows the comparison with a conventional approach.

In section II, first we briefly review the formal theory of photon scattering, the low energy limit of the scattering amplitude and the concept of generalized polarizabilities as basic quantities. Then we develop the general formalism of how these polarizabilities can be calculated by the LIT method. The application of this method on the deuteron as a test case is described in section III. For demonstrating the method it suffices to limit the explicit calculation to the low energy regime where the E1 contribution dominates. The results are presented and discussed in section IV where we also give a summary and an outlook.

II. FORMAL DEVELOPMENTS

We start the formal part with a short resume of the salient features of photon scattering off a bound many-body system (for a more detailed review see e.g. [12]), i.e. we consider the process

$$\gamma(\vec{k}) + N_i(\vec{P}_i) \longrightarrow \gamma(\vec{k}') + N_f(\vec{P}_f), \quad (1)$$

for an incoming photon with momentum \vec{k} and polarization \vec{e}_λ and an outgoing photon with momentum \vec{k}' and polarization $\vec{e}'_{\lambda'}$, while the system makes a transition from an initial state with total momentum \vec{P}_i and intrinsic state

$|i\rangle$ to a final state with total momentum \vec{P}_f with intrinsic state state $|f\rangle$.

A. The photon scattering amplitude

In view of the weakness of the electromagnetic interaction one can apply perturbation methods. In the lowest, i.e. second order in the e.m. coupling, the scattering amplitude is given by two terms, the contact or two photon amplitude (TPA) $B_{\lambda'\lambda}(\vec{k}', \vec{k})$ and the resonance amplitude (RA) $R_{\lambda'\lambda}(\vec{k}', \vec{k})$. A graphical illustration is shown in Fig. 1.

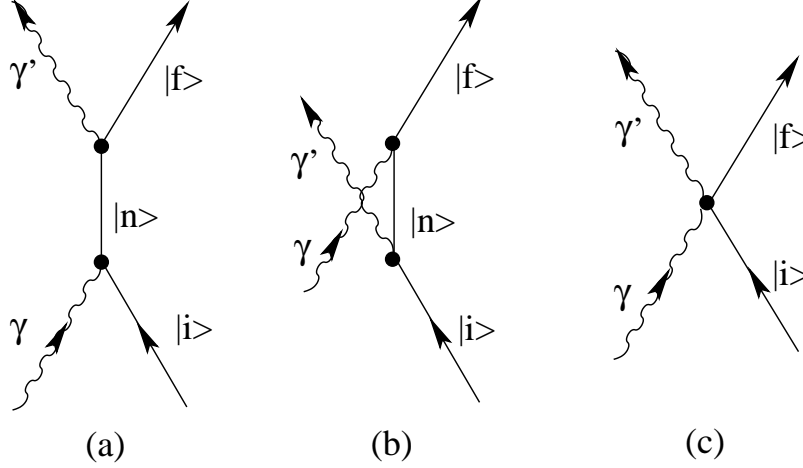


FIG. 1: Diagrammatic representation of the resonance (direct (a) and crossed (b)) and the two-photon amplitude (c) for photon scattering.

Accordingly, the total scattering amplitude is the sum of these two contributions

$$T_{\lambda'\lambda}^{fi}(\vec{k}', \vec{k}) = B_{\lambda'\lambda}^{fi}(\vec{k}', \vec{k}) + R_{\lambda'\lambda}^{fi}(\vec{k}', \vec{k}), \quad (2)$$

where the two-photon amplitude as depicted in diagram (c) of Fig. 1 has the form

$$B_{\lambda'\lambda}^{fi}(\vec{k}', \vec{k}) = -\langle f | \int d^3x d^3y e^{i\vec{k}' \cdot \vec{x}} e^{-i\vec{k} \cdot \vec{y}} \vec{e}_{\lambda'}^{*} \cdot \overleftrightarrow{B}(\vec{x}, \vec{y}) \cdot \vec{e}_{\lambda} | i \rangle, \quad (3)$$

and the resonance amplitude (RA) (diagrams (a) and (b) of Fig. 1) is given by

$$R_{\lambda'\lambda}^{fi}(\vec{k}', \vec{k}) = \langle f | \left[\vec{e}_{\lambda'}^{*} \cdot \vec{J}(-\vec{k}', 2\vec{P}_f + \vec{k}') G(k + i\epsilon) \vec{e}_{\lambda} \cdot \vec{J}(\vec{k}, 2\vec{P}_i + \vec{k}) \right. \\ \left. + \vec{e}_{\lambda} \cdot \vec{J}(\vec{k}, 2\vec{P}_f - \vec{k}) G(-k' + i\epsilon) \vec{e}_{\lambda'}^{*} \cdot \vec{J}(-\vec{k}', 2\vec{P}_i - \vec{k}') \right] | i \rangle, \quad (4)$$

with the intermediate propagator

$$G(z) = (H - E_i - z)^{-1}. \quad (5)$$

In these expressions, the c.m. motion has been separated applying translation invariance. Thus the initial and final states refer to the intrinsic motion of the many-particle system only. In principle, the Hamiltonian H and the energy E_i contain contributions from the c.m. motion. Furthermore, the splitting in a resonance and a two-photon amplitude is gauge dependent. This gauge dependence is reflected in the gauge conditions sketched briefly below.

The cartesian tensor operator \overleftrightarrow{B} of rank 2 in Eq. (3) represents the second order term of the e.m. interaction with the system under consideration, and the current operator in Eq. (4)

$$\vec{J}(\vec{k}, \vec{P}) = \vec{j}(\vec{k}) + \frac{\vec{P}}{2AM} \rho(\vec{k}) \quad (6)$$

acts on the intrinsic variables of the system only. It consists of the intrinsic current $\vec{j}(\vec{k})$ plus a term taking into account the convection current of the separated c.m. motion. M denotes the nucleon mass and A the mass number of the nucleus. The intrinsic charge and current operators consist of a kinetic or one-body and a meson exchange part

$$\rho(\vec{k}) = \rho_{[1]}(\vec{k}) + \rho_{[2]}(\vec{k}), \quad (7)$$

$$\vec{j}(\vec{k}) = \vec{j}_{[1]}(\vec{k}) + \vec{j}_{[2]}(\vec{k}), \quad (8)$$

with

$$\rho_{[1]}(\vec{k}) = \sum_l e_l e^{-i\vec{k}\cdot\vec{r}_l}, \quad (9)$$

$$\vec{j}_{[1]}(\vec{k}) = \frac{1}{2M} \sum_l \left(e_l \{ \vec{p}_l, e^{-i\vec{k}\cdot\vec{r}_l} \} + \mu_l \vec{\sigma}_l \times \vec{k} e^{-i\vec{k}\cdot\vec{r}_l} \right). \quad (10)$$

Here, e_l and μ_l denote charge and magnetic moment of the l -th particle and \vec{p}_l and $\vec{\sigma}_l$ its internal momentum and spin operator. The expressions for the corresponding exchange operators depend on the interaction model. At least in the nonrelativistic limit, the exchange contribution to the charge density vanishes (Siegert's hypothesis). Furthermore, also the TPA consists of a kinetic one-body contribution and a two-body exchange amplitude

$$\overset{\leftrightarrow}{B}(\vec{k}', \vec{k}) = \overset{\leftrightarrow}{B}_{[1]}(\vec{k}', \vec{k}) + \overset{\leftrightarrow}{B}_{[2]}(\vec{k}', \vec{k}), \quad (11)$$

where the kinetic one-body operator is given by

$$\overset{\leftrightarrow}{B}_{[1]}(\vec{k}', \vec{k}) = -\frac{1}{M} \sum_l e_l^2 e^{-i(\vec{k}-\vec{k}')\cdot\vec{r}_l}, \quad (12)$$

which is the sum of the individual Thomson amplitudes.

Gauge invariance of the electromagnetic interaction leads to gauge conditions for the various e.m. operators according to

$$\vec{k} \cdot \vec{j}(\vec{k}) = [H, \rho(\vec{k})], \quad (13)$$

$$\vec{k}' \cdot \overset{\leftrightarrow}{B}(\vec{k}', \vec{k}) = [\rho(-\vec{k}'), \vec{j}(\vec{k})], \quad (14)$$

where $H = T + V$ denotes the intrinsic Hamiltonian of the nuclear system with T as kinetic energy and the interaction potential V . Separating the one-body and exchange contributions, one finds

$$\vec{k} \cdot \vec{j}_{[1]}(\vec{k}) = [T, \rho_{[1]}(\vec{k})], \quad (15)$$

$$\vec{k} \cdot \vec{j}_{[2]}(\vec{k}) = [V, \rho_{[1]}(\vec{k})] + [T, \rho_{[2]}(\vec{k})], \quad (16)$$

$$\vec{k}' \cdot \overset{\leftrightarrow}{B}_{[1]}(\vec{k}', \vec{k}) = [\rho_{[1]}(-\vec{k}'), \vec{j}_{[1]}(\vec{k})], \quad (17)$$

$$\vec{k}' \cdot \overset{\leftrightarrow}{B}_{[2]}(\vec{k}', \vec{k}) = [\rho_{[1]}(-\vec{k}'), \vec{j}_{[2]}(\vec{k})] + [\rho_{[2]}(-\vec{k}'), \vec{j}_{[1]}(\vec{k})]. \quad (18)$$

One important consequence are the low energy limits [13, 14]

$$\vec{j}(0) = [H, \vec{D}], \quad (19)$$

$$B_{[1],\lambda'\lambda}^{ii}(0,0) = -\vec{e}_{\lambda'}^* \cdot \vec{e}_\lambda \frac{Ze^2}{M}, \quad (20)$$

$$B_{[2],\lambda'\lambda}^{ii}(0,0) = -\langle i | [\vec{e}_{\lambda'}^* \cdot \vec{D}, [V, \vec{e}_\lambda \cdot \vec{D}]] | i \rangle, \quad (21)$$

$$R_{\lambda'\lambda}^{ii}(0,0) = \vec{e}_{\lambda'}^* \cdot \vec{e}_\lambda \frac{NZe^2}{AM} - B_{[2],\lambda'\lambda}^{ii}(0,0), \quad (22)$$

resulting in the low energy limit for the total scattering amplitude

$$T_{\lambda'\lambda}^{ii}(0,0) = -\vec{e}_{\lambda'}^* \cdot \vec{e}_\lambda \frac{(Ze)^2}{AM}, \quad (23)$$

which is the classical Thomson limit.

B. Generalized nuclear polarizabilities

The expansion of the scattering amplitude with respect to the total angular momentum transferred to the nucleus in the scattering process leads to the concept of generalized polarizabilities. These polarizabilities allow in a convenient manner to separate geometrical aspects related to the angular momentum properties and dynamical effects given by the strength of the various polarizabilities. To this end, one starts from the multipole expansion of the plane wave (see, e.g. [15])

$$\vec{e}_\lambda e^{i\vec{k}\cdot\vec{r}} = -\sqrt{2\pi} \sum_{LM} \hat{L} D_{M\lambda}^L(R) \sum_{\nu=0,1} \lambda^\nu \vec{A}_M^L(M^\nu; k), \quad (24)$$

with standard electric and magnetic multipole fields $\vec{A}_M^L(M^\nu; k)$, where ν indicates the type of multipole field ($M^0 = E$ (electric) and $M^1 = M$ (magnetic)). Then one expands the current operator in terms of electric ($M^{0,L} = E^L$) and magnetic ($M^{1,L} = M^L$) multipole operators

$$\vec{e}_\lambda \cdot \vec{j}(\vec{k}) = -\sqrt{2\pi} \sum_{LM} \hat{L} D_{M\lambda}^L(R) \sum_{\nu=0,1} \lambda^\nu M_M^{\nu,L}, \quad (25)$$

where R denotes a rotation which carries the quantization axis into the direction of \vec{k} , and $D_{M\lambda}^L$ denotes the corresponding rotation matrix [15]. A similar expansion holds for the two-photon operator.

The electric and magnetic multipole fields of order L of the incoming photon transfer an angular momentum L according to the strengths of the corresponding nuclear transition multipole moments. Similarly, the scattered photon transfers angular momentum L' . These consecutive momentum transfers can further be classified according to the total momentum transfer J to the nucleus with $|L - L'| \leq J \leq L + L'$. The corresponding strength is given by the polarizability

$$P_{if,J}^{L'L\lambda\lambda'}(k', k) = \sum_{\nu'\nu=0,1} \lambda'\nu' \lambda^\nu P_{if,J}(M^{\nu'}L', M^\nu L, k', k), \quad (26)$$

where ν classifies the type of multipole transition as already mentioned. A graphical visualization of the generalized polarizability is shown in Fig. 2.

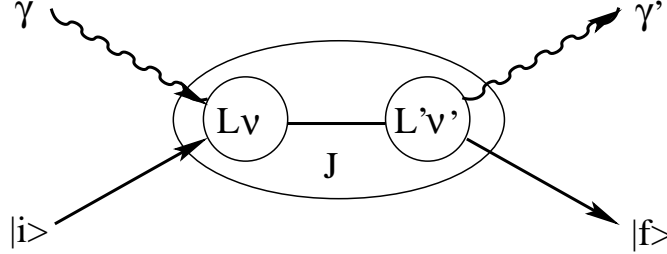


FIG. 2: Graphical representation of the contribution of the direct term of the resonance amplitude to the generalized polarizability $P_{if,J}(M^{\nu'}L', M^\nu L, k', k)$ with consecutive angular momentum transfers L and L' by multipoles of type ν and ν' , respectively, coupled to total angular momentum transfer J .

Then the expansion of the total scattering amplitude in terms of these polarizabilities reads

$$T_{\lambda'\lambda}^{fi}(\vec{k}', \vec{k}) = (-)^{1+\lambda'+I_f-M_i} \sum_{L',M',L,M,J} (-)^{L+L'} (2J+1) \begin{pmatrix} I_f & J & I_i \\ -M_f & m & M_i \end{pmatrix} \begin{pmatrix} L & L' & J \\ M & M' & -m \end{pmatrix} \times P_{if,J}^{L'L\lambda\lambda'}(k', k) D_{M,\lambda}^L(R) D_{M',-\lambda'}^{L'}(R'), \quad (27)$$

where (I_i, M_i) and (I_f, M_f) refer to the angular momenta and their projections on the quantization axis of the initial and final states, respectively. Furthermore, R and R' describe the rotations which carry the quantization axis into the directions of the photon momenta \vec{k} and \vec{k}' , respectively, and $D_{M,\lambda}^L(R)$ and $D_{M',-\lambda'}^{L'}(R')$ the corresponding rotation matrices in the convention of Rose [15].

As for the scattering amplitude, the polarizabilities can be separated in a TPA and a resonance contribution

$$P_{if,J}(M^{\nu'}L', M^\nu L, k', k) = P_{if,J}^{TPA}(M^{\nu'}L', M^\nu L, k', k) + P_{if,J}^{\text{res}}(M^{\nu'}L', M^\nu L, k', k), \quad (28)$$

where for the resonance amplitude one has

$$P_{i_f, J}^{\text{res}}(M^{\nu'} L', M^{\nu} L, k', k) = 2\pi(-)^{L+J} \frac{\hat{L}\hat{L}'}{\hat{J}} \times \langle I_f E_f | \left(\left[M^{\nu', L'}(k') G(k + i\varepsilon) M^{\nu, L}(k) \right]^J + \left[M^{\nu, L}(k) G(-k' + i\varepsilon) M^{\nu', L'}(k') \right]^J \right) | I_i E_i \rangle. \quad (29)$$

Here the symbol “[...]”^J means that the two multipole operators are coupled to a spherical tensor of rank J . Furthermore, we have neglected the small c.m. current contribution of Eq. (6). The two-photon contribution to the polarizability is given by

$$P_{i_f, J}^{\text{TPA}}(M^{\nu', L'}, M^{\nu, L}, k', k) = 2\pi(-)^{L+J+1} \frac{\hat{L}\hat{L}'}{\hat{J}} \langle I_f E_f | \int d^3x d^3y \left[\vec{A}^{L'}(M^{\nu'}; k, \vec{x}) \cdot \overset{\leftrightarrow}{B}(\vec{x}, \vec{y}) \cdot \vec{A}^L(M^{\nu}; k, \vec{y}) \right]^J | I_i E_i \rangle. \quad (30)$$

The evaluation of the TPA contribution to the polarizabilities is straightforward once the TPA operator $\overset{\leftrightarrow}{B}(\vec{x}, \vec{y})$ is given.

For the resonance contribution, one finds by evaluating the reduced matrix element in standard fashion (see e.g. [16])

$$P_{i_f, J}^{\text{res}}(M^{\nu'} L', M^{\nu} L, k', k) = 2\pi(-)^{L+I_f+I_i} \hat{L}\hat{L}' \times \sum_{E_n, I_n} \left[\left\{ \begin{matrix} L & L' & J \\ I_f & I_i & I_n \end{matrix} \right\} \frac{\langle I_f E_f | M^{\nu', L'}(k') | I_n E_n \rangle \langle I_n E_n | M^{\nu, L}(k) | I_i E_i \rangle}{E_n - E_i - k - i\varepsilon} + (-)^{L+L'+J} \left\{ \begin{matrix} L' & L & J \\ I_f & I_i & I_n \end{matrix} \right\} \frac{\langle I_f E_f | M^{\nu, L}(k) | I_n E_n \rangle \langle I_n E_n | M^{\nu', L'}(k') | I_i E_i \rangle}{E_n - E_i + k' - i\varepsilon} \right]. \quad (31)$$

Obviously, the calculation of the resonance part is more involved because of the summation over all possible intermediate states $|I_n\rangle$ and energies E_n .

The low energy expansion of the polarizabilities has been discussed in Ref. [14]. For $k = 0$ only the scalar E1-polarizability is nonvanishing, i.e.

$$P_J(E1, E1)|_{k=0} = -\delta_{J0} \hat{I} \sqrt{3} \frac{e^2 Z^2}{M_A}, \quad (32)$$

with I as ground state spin, which corresponds to the Thomson amplitude.

C. The scattering cross section

Before turning to the LIT method, we will briefly review the scattering cross section in terms of the polarizabilities. For unpolarized photon and target it is given by

$$\frac{d\sigma}{d\Omega} = \frac{k'}{k} \frac{c(\vec{k}, \vec{p}_i, k')}{2(2I_i + 1)} \sum_{\lambda, \lambda', M_i, M_f} |T_{\lambda' \lambda, M_f, M_i}^{f i}(\vec{k}', \vec{k})|^2, \quad (33)$$

with a kinematic factor resulting from the final state phase space and the incoming flux factor

$$c(\vec{k}, \vec{p}_i, k') = \frac{\omega + E_i - \omega'}{(\omega + E_i) \left| \frac{\vec{k}}{\omega} - \frac{\vec{p}_i}{E_i} \right|}. \quad (34)$$

In terms of the polarizabilities one finds for the cross section [17, 18]

$$\frac{d\sigma}{d\Omega} = \frac{k'}{k} \frac{c(\vec{k}, \vec{p}_i, k')}{2I_i + 1} \sum_{L', L, K', K, J} \sum_{\nu', \nu, \bar{\nu}', \bar{\nu}} P_{i_f, J}(M^{\nu'} L', M^{\nu} L) P_{i_f, J}^*(M^{\bar{\nu}'} K', M^{\bar{\nu}} K) g_J^{\nu' L' \nu L \bar{\nu}' K' \bar{\nu} K}(\theta), \quad (35)$$

where the angular functions are given by

$$g_J^{\nu' L' \nu L \bar{\nu}' K' \bar{\nu} K}(\theta) = \frac{(-)^J}{2} (2J+1) (-)^{L+K+\nu'+\bar{\nu}'} \sum_j (2j+1) (1+(-)^{L+K+j+\nu+\bar{\nu}}) (1+(-)^{L'+K'+j+\nu'+\bar{\nu}'}) \\ \times \begin{pmatrix} L' & K' & j \\ 1 & -1 & 0 \end{pmatrix} \begin{pmatrix} L & K & j \\ 1 & -1 & 0 \end{pmatrix} \left\{ \begin{matrix} L & K & j \\ K' & L' & J \end{matrix} \right\} P_j(\cos \theta), \quad (36)$$

with $P_j(\cos \theta)$ as Legendre polynomials. For pure $E1$ transitions one obtains

$$\frac{d\sigma(E1)}{d\Omega} = \frac{k'}{k} \frac{c(\vec{k}, \vec{p}_i, k')}{(2I_i+1)} \sum_J |P_{if,J}(E1, E1)|^2 g_J^{E1}(\theta), \quad (37)$$

where in an abbreviated notation

$$g_0^{E1}(\theta) = \frac{1}{6} (1 + \cos^2 \theta), \quad (38)$$

$$g_1^{E1}(\theta) = \frac{1}{4} (2 + \sin^2 \theta), \quad (39)$$

$$g_2^{E1}(\theta) = \frac{1}{12} (13 + \cos^2 \theta). \quad (40)$$

D. Application of the Lorentz integral transform method

A convenient method for the evaluation of the polarizabilities is provided by the Lorentz Integral Transform (LIT) [9] as applied to exclusive reactions. For this purpose we separate in Eq. (29) the intermediate propagator from the reduced matrix element by writing

$$G(k+i\epsilon) = \int_{E_0}^{\infty} dE \frac{\delta(H-E)}{E-E_i-k-i\epsilon}, \quad (41)$$

where E_0 denotes the ground state energy, and introduce for the separated reduced matrix element as a convenient abbreviation a quantity which henceforth will be called the polarizability strength function

$$F_{(\nu' L', \nu L)J}^{I_f I_i}(k', k, E) = \frac{(-)^{J+I_f+I_i}}{\hat{J}} \langle I_f E_f || [M^{\nu', L'}(k') \times \delta(H-E) M^{\nu, L}(k)]^J || I_i E_i \rangle. \quad (42)$$

One should note that in general the strength function is off energy shell, i.e. $E \neq E_i + k$. Evaluating the reduced matrix element, one obtains

$$F_{(\nu' L', \nu L)J}^{I_f I_i}(k', k, E) = \sum_{I_n} \rho(I_n, E) \left\{ \begin{matrix} L & L' & J \\ I_f & I_i & I_n \end{matrix} \right\} \langle I_f E_f || M^{\nu', L'}(k') || I_n, E \rangle \langle I_n, E || M^{\nu, L}(k) || I_i E_i \rangle, \quad (43)$$

with $\rho(I, E)$ as density of states for a given energy E and angular momentum I . In terms of the strength functions the polarizability becomes

$$P_{if,J}^{\text{res}}(M^{\nu'} L', M^{\nu} L, k', k) = 2\pi (-)^{L+I_f+I_i} \hat{L} \hat{L}' \\ \times \int_{E_0}^{\infty} dE \left[\frac{F_{(\nu' L', \nu L)J}^{I_f I_i}(k', k, E)}{E-E_i-k-i\epsilon} + (-)^{L+L'+J} \frac{F_{(\nu L, \nu' L')J}^{I_f I_i}(k, k', E)}{E-E_i+k'-i\epsilon} \right]. \quad (44)$$

One can separate the real and imaginary parts of the propagator according to

$$(P_{if,J}^{\text{res}}(M^{\nu'} L', M^{\nu} L, k', k))_{\text{Re}} = 2\pi (-)^{L+I_f+I_i} \hat{L} \hat{L}' \\ \times \mathcal{P} \int_{E_0}^{\infty} dE \left[\frac{F_{(\nu' L', \nu L)J}^{I_f I_i}(k', k, E)}{E-E_i-k} + (-)^{L+L'+J} \frac{F_{(\nu L, \nu' L')J}^{I_f I_i}(k, k', E)}{E-E_i+k'} \right], \quad (45)$$

where \mathcal{P} stands for the principal value of the integral, and

$$(P_{if,J}^{\text{res}}(M^{\nu'}L', M^{\nu}L, k', k))_{\text{Im}} = 2\pi^2(-)^{L+I_f+I_i}\hat{L}\hat{L}' \times \left[F_{(\nu'L',\nu L),J}^{I_f I_i}(k', k, E_i + k) + (-)^{L+L'+J} F_{(\nu L, \nu' L'),J}^{I_f I_i}(k, k', E_i - k') \right]. \quad (46)$$

where the second term contributes only if $E_i > E_0$, i.e. if the initial state is an excited state. The subscripts ‘‘Re’’ and ‘‘Im’’ indicate the contributions of the real and imaginary parts of the propagator, respectively. For elastic scattering the strength function is real and then Eqs. (45) and (46) represent the real and imaginary parts, respectively, of the polarizability.

The strength functions are the principal quantities which are determined by the Lorentz Integral Transform method. Thus the main task is the evaluation of the strength function $F_{(\nu'L',\nu L),J}^{I_f I_i}(k', k, E)$. To this end we first consider the following partial strength function for a fixed intermediate total angular momentum state $|I_n M_n\rangle$ as defined by

$$F_{\nu'L',\nu L}^{I_f I_i; I_n}(k', k, E) = \rho(I_n, E) \langle I_f E_f || M^{\nu', L'}(k') || I_n, E \rangle \langle I_n, E || M^{\nu, L}(k) || I_i E_i \rangle. \quad (47)$$

In terms of these partial strength functions the polarizability strength is given by

$$F_{(\nu'L',\nu L),J}^{I_f I_i}(k', k, E) = \sum_{I_n} \left\{ \begin{matrix} L & L' & J \\ I_f & I_i & I_n \end{matrix} \right\} F_{\nu'L',\nu L}^{I_f I_i; I_n}(k', k, E). \quad (48)$$

The partial strength can be expressed in terms of states of good total angular momentum I_n which are generated by the action of a multipole operator $M^{\nu L}$ on a state ψ^I with good angular momentum I according to

$$|(M^{\nu, L}(k) \times \psi^I)_{I_n M_n}\rangle = \left[M^{\nu, L}(k) \times |I\rangle \right]_{M_n}^{I_n}. \quad (49)$$

Namely, using

$$\begin{aligned} \langle IM | (M^{\nu, L}(k) \times \psi^{I_i})_{I_n M_n} \rangle &= \sum_{M M_i} (-)^{I_i - L - M_n} \hat{I}_n \begin{pmatrix} L & I_i & I_n \\ M & M_i & -M_n \end{pmatrix} \langle IM | M_M^{\nu L} | I_i M_i \rangle \\ &= \delta_{I I_n} \delta_{M M_n} \frac{(-)^{I_i - I_n - L}}{\hat{I}_n} \langle I_n || M^{\nu L} || I_i \rangle, \end{aligned} \quad (50)$$

one finds

$$F_{\nu'L',\nu L}^{I_f I_i; I_n}(k', k, E) = (-)^{I_n - I_i + L - L' + \nu'} \sum_{M_n} \langle (M^{\nu', L'}(k) \times \psi^{I_f})_{I_n M_n} | \delta(H - E) | (M^{\nu, L}(k) \times \psi^{I_i})_{I_n M_n} \rangle. \quad (51)$$

Then we perform a Lorentz integral transform with a complex argument $\sigma = \sigma_R + i\sigma_I$

$$L_{\nu'L',\nu L}^{I_f I_i; I_n}(k', k, \sigma) = \int_{E_0}^{\infty} dE \frac{F_{\nu'L',\nu L}^{I_f I_i; I_n}(k', k, E)}{(E - \sigma)(E - \sigma^*)}. \quad (52)$$

Inserting the explicit form for the strength function of Eq. (51) and integrating over the δ -function, one finds consecutively

$$\begin{aligned} L_{\nu'L',\nu L}^{I_f I_i; I_n}(k', k, \sigma) &= (-)^{I_n - I_i + L - L' + \nu'} \\ &\times \sum_{M_n} \langle (M^{\nu', L'}(k) \times \psi^{I_f})_{I_n M_n} | (H - \sigma)^{-1} (H - \sigma^*)^{-1} | (M^{\nu, L}(k) \times \psi^{I_i})_{I_n M_n} \rangle \\ &= (-)^{I_n - I_i + L - L' + \nu'} \rho(I_n, \sigma) \sum_{M_n} \langle \tilde{\psi}_{I_f; I_n M_n}^{\nu', L'}(k', \sigma) | \tilde{\psi}_{I_i; I_n M_n}^{\nu, L}(k, \sigma) \rangle, \end{aligned} \quad (53)$$

where $\rho(I_n, \sigma)$ takes into account the possibility, that for the given I_n and σ several Lorentz states may exist. Here, the Lorentz state of good total angular momentum I_n and projection M_n obeys the equation

$$(H - \sigma^*) | \tilde{\psi}_{I_i; I_n M_n}^{\nu, L}(k, \sigma) \rangle = | (M^{\nu, L}(k) \times \psi^{I_i})_{I_n M_n} \rangle. \quad (54)$$

After inversion of the Lorentz transform, one obtains the desired polarizability strength function from Eq. (48) which then serves for the evaluation of the appropriate generalized polarizability.

III. THE DEUTERON CASE

For the calculation of deuteron elastic photon scattering the γ -deuteron c.m.-system is chosen, where one has $k = k'$. In order to demonstrate the LIT method it suffices to consider the at low energies dominant $E1$ transitions with the $E1$ operator in the long wave length approximation (Siegert form)

$$E_M^1 = i[H, D_M^1], \text{ where } D_M^1 = \frac{\sqrt{\alpha}}{3\sqrt{2}} r Y_{1M}(\Omega) \quad (55)$$

is independent of k . Here α denotes the fine structure constant, and (r, Ω) represents the relative neutron-proton coordinate. Furthermore, H denotes the intrinsic two-nucleon hamiltonian containing the nucleon-nucleon interaction. The small c.m. contribution to the Hamiltonian is neglected for simplicity. Due to the dipole approximation only the polarizabilities $P_J(E1, k)$ ($J = 0, 1, 2$, in an abbreviated notation) contribute. Instead of the corresponding partial $E1$ -strength function

$$\begin{aligned} F_{E1, E1}^{11;j}(E) &= (-)^{j-1} \sum_m \langle ([D^1, H] \times \psi_d^1) j m | \delta(H - E) | ([D^1, H] \times \psi_d^1) j m \rangle \\ &= (-)^{j-1} (E - E_0)^2 \sum_m \langle (D^1 \times \psi_d^1) j m | \delta(H - E) | (D^1 \times \psi_d^1) j m \rangle, \end{aligned} \quad (56)$$

where E_0 denotes the ground state energy, we will consider the reduced partial strength function

$$\begin{aligned} \tilde{F}_{E1, E1}^{11;j}(E) &= \frac{F_{E1, E1}^{11;j}(E)}{(E - E_0)^2} \\ &= (-)^{j-1} \sum_m \langle (D^1 \times \psi_d^1) j m | \delta(H - E) | (D^1 \times \psi_d^1) j m \rangle. \end{aligned} \quad (57)$$

One should note that $\tilde{F}_{E1, E1}^{11;j}$ is independent of k . The associated Lorentz state obeys as LIT equation (see Eq. (54))

$$(H - \sigma^*) |\tilde{\psi}_{jm}(\sigma)\rangle = |(D^1 \times \psi_d^1) j m\rangle, \quad (58)$$

which is independent of k . The Lorentz state can be expanded into partial waves according to the orbital angular momentum l

$$\langle r, \Omega | \tilde{\psi}_{jm}(\sigma) \rangle = \frac{\sqrt{\alpha}}{r\sqrt{4\pi}} \sum_{l=|j-1|}^{j+1} \Phi_{jl}(\sigma, r) \langle \Omega | (l1) j m \rangle, \quad (59)$$

where $|(l1) j m\rangle$ represents the spin-angular state of orbital angular momentum l coupled with total spin-one to a total angular momentum j , and the matrix element refers to spin and angular degrees of freedom only. The state $\tilde{\psi}_{jm}(\sigma)$ generates the LIT $\tilde{L}_{E1, E1}^{11;j}$ of the reduced strength $\tilde{F}_{E1, E1}^{11;j}$.

Inserting the expansion of $\tilde{\psi}_{jm}$ into Eq. (58) and projecting onto a state $|(l1) j m\rangle$, one finds a set of radial differential equations

$$\left[-\frac{\hbar^2}{M} \left(\frac{d^2}{dr^2} - \frac{l(l+1)}{r^2} \right) - \sigma^* \right] \Phi_{jl}(\sigma, r) + \sum_{l'} V_{jl, j'l'} \Phi_{j'l'}(\sigma, r) = \frac{1}{3\sqrt{2}} r f_{jl}(r) \quad (60)$$

with

$$f_{jl}(r) = \delta_{l1} u(r) + (-)^{j+1} 3\sqrt{5} \hat{l} \begin{pmatrix} 2 & 1 & l \\ 0 & 0 & 0 \end{pmatrix} \begin{Bmatrix} 2 & 1 & 1 \\ j & 1 & l \end{Bmatrix} w(r), \quad (61)$$

where $u(r)$ and $w(r)$ are the deuteron radial s - and d -wave functions. Two of them are uncoupled (${}^3P_0 : l = 1, j = 0$; ${}^3P_1 : l = 1, j = 1$) and one is coupled (${}^3P_2 - {}^3F_2 : l_1 = 1, l_2 = 3, j = 2$). Equation (60) is very similar to a radial Schrödinger equation, but with a complex energy σ and an additional source term on the right-hand side.

For convenience we introduce the following three reduced LITs

$$L_j(\sigma) := (-)^{j-1} \frac{4\pi}{2j+1} \tilde{L}_{E1, E1}^{11;j}(\sigma) = \frac{4\pi}{2j+1} \sum_m \langle \tilde{\psi}_{jm}(\sigma) | \tilde{\psi}_{jm}(\sigma) \rangle = \alpha \sum_l \int_0^\infty |\Phi_{jl}(\sigma, r)|^2 dr, \quad (62)$$

and corresponding reduced strength $F_j(E) = \tilde{F}_{E_1, E_1}^{11;j}(E)/(2j+1)$. Then the polarizability strength function becomes

$$F_{E_1, E_1}^{11;j}(E) = \frac{(E - E_0)^2}{4\pi} \sum_j (-)^{j+1} (2j+1) \begin{Bmatrix} 1 & 1 & J \\ 1 & 1 & j \end{Bmatrix} F_j(E), \quad (63)$$

and, according to Eq. (46), the $E1$ polarizabilities are given by

$$\begin{aligned} (P_J^{\text{res}}(E1, k))_{Im} &= -6\pi^2 F_{E_1, E_1}^{11;j}(k + E_0) \\ &= \frac{3}{2}\pi k^2 \sum_j (-)^j (2j+1) \begin{Bmatrix} 1 & 1 & J \\ 1 & 1 & j \end{Bmatrix} F_j(k + E_0), \end{aligned} \quad (64)$$

$$\begin{aligned} (P_J^{\text{res}}(E1, k))_{Re} &= \frac{3}{2} \sum_j (-)^j (2j+1) \begin{Bmatrix} 1 & 1 & J \\ 1 & 1 & j \end{Bmatrix} \mathcal{P} \int dE (E - E_0)^2 F_j(E) \left(\frac{1}{E - E_0 - k} + \frac{(-)^J}{E - E_0 + k} \right) \\ &= \frac{1}{\pi} \mathcal{P} \int dk' (P_J^{\text{res}}(E1, k'))_{Im} \left(\frac{1}{k' - k} + \frac{(-)^J}{k' + k} \right). \end{aligned} \quad (65)$$

The latter expression for the real part corresponds to the dispersion theoretic approach of Ref. [1]. It is a consequence of the fact, that in this special case of taking the $E1$ -operator in the low energy limit the polarizability strength $F_{E_1, E_1}^{11;j}$ becomes independent of the photon momentum k . However, in general this is not true.

IV. RESULTS AND DISCUSSION

For the numerical solution of the radial equation (60) for the radial Lorentz states $\Phi_{jl}(\sigma, r)$ we have chosen the Argonne potential AV18 [19] as interaction model. The resulting three $L_j(\sigma)$ are shown in Fig. 3 for a constant

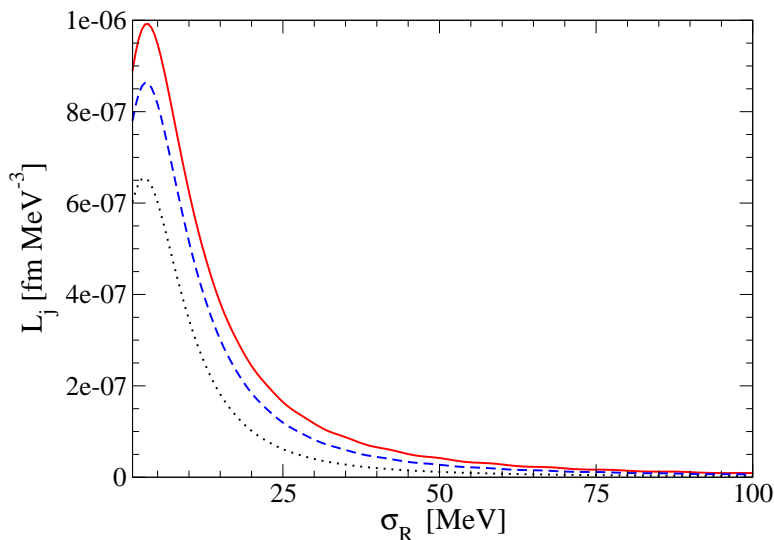


FIG. 3: (Color online) Lorentz integral transforms $L_j(\sigma)$ with $\sigma_I = 5$ MeV: $j = 0$ (dotted), $j = 1$ (solid), $j = 2$ (dashed).

$\sigma_I = 5$ MeV as function of σ_R up to 100 MeV. The figure shows that the three LITs have quite a similar behavior. All three exhibit a pronounced peak in the low σ_R region, only the peak heights are slightly different. For the principal value integral in (45) also high-energy contributions could play an important role, therefore we illustrate in Fig. 4 the transforms in an extended σ_R range. One finds that the behavior at high σ_R is approximately described by σ_R^{-2} . It shows that at large σ_R the transforms are dominated by low-energy contributions. In fact, for the extreme case of a δ -strength, i.e. $F(E) = F_0 \delta(E - E_0)$, one obtains $L(\sigma) = F_0 / ((\sigma_R - E_0)^2 + \sigma_I^2)$.

One also notices in Fig. 4 the onset of oscillations at higher σ_R , which are more pronounced for L_1 and L_2 . The origin of these oscillations lies in the relatively small value of 5 MeV for σ_I , which makes a high-precision solution of (60) with increasing σ_R more and more difficult. Such a small σ_I value, however, is advantageous in the low σ_R region, where (i) it does not lead to numerical problems and (ii) prominent structures of a small width could be present, e.g.,

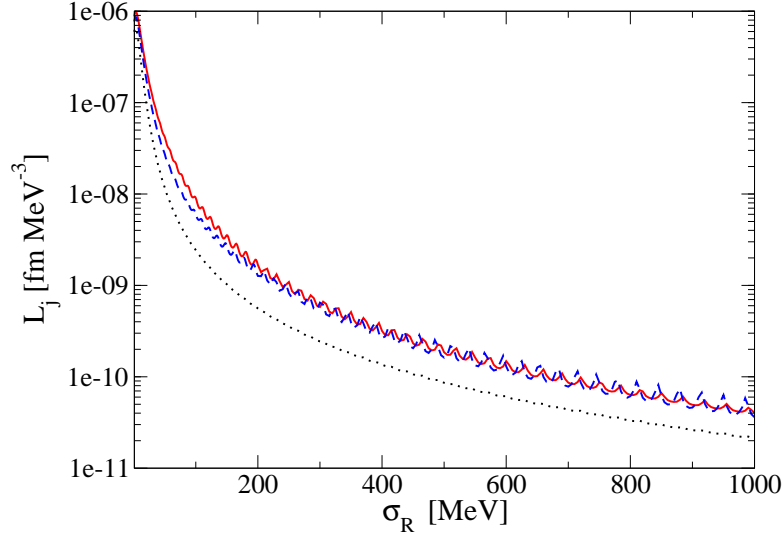


FIG. 4: (Color online) As in Fig. 3, but for an extended range of σ_R .

a low-energy peak. The small σ_I value will then allow one to resolve such details and nonetheless will not lead to problems for the reconstruction of the high-energy strength, since structures with a small width are not present at higher energies. One could also completely avoid the oscillations at higher σ_R by choosing a transform with different σ_I values for low- and high-energy regions, as has been done in [20].

In order to obtain the strength function $F_j(E)$ one has to invert the integral transforms L_j defined in (62). Details about the inversion of the LIT are found in [9, 21], and further, more general inversion aspects are discussed in [22]. Accordingly, we use expansions of the calculated LITs, $L_j(\sigma_R, \sigma_I = 5\text{MeV})$, in a set of basis functions $\tilde{\chi}_n^{(1)}$ ($n = 1, 2, \dots, N$), where the expansion coefficients are determined by a best fit. Here we take, as in [9], the set (for fixed σ_I)

$$\tilde{\chi}_n^{(1)}(\sigma_R) = \int_0^\infty dE \frac{\chi_n^{(1)}(E)}{(E - \sigma_R)^2 + \sigma_I^2} \quad (66)$$

with

$$\chi_n^{(1)}(E) = E^{\alpha_1} \exp\left(-\frac{\alpha_2 E}{n\beta}\right), \quad (67)$$

where α_i and β are nonlinear parameters. The inversion results, $F_j(E)$, are shown in Fig. 5. One observes pronounced low-energy peaks with a strong subsequent fall-off which becomes weaker at somewhat higher energies. The fall-off becomes stronger again at even higher energies, namely beyond about 200 MeV (300 MeV) in case of F_0 ($F_{1/2}$). As a matter of fact, the inversion results are already not very good somewhat below those energies, since there we do not find, as it would be necessary, a stability for the inversion solutions for a limited range of the number of basis functions N . The origin of this problematic high-energy behavior lies in the choice of basis functions. By construction they all have an exponential high-energy fall-off and thus are not suitable to describe a function with a different high-energy behavior, since N cannot be increased arbitrarily because of the numerical accuracy of the transform to be fitted.

As already mentioned, for the principal value integral in (45) also high-energy contributions of the strength function could matter. Therefore it is better to search for a basis set which does not have the shortcomings of the set in (67), but which is more appropriate to describe the strength function over a much larger energy range, even if it could lead to a somewhat less precise inversion at lower energies. For this purpose we introduce an alternative set without an exponential fall-off:

$$\chi_n^{(2)} = E^{\alpha_n(E)} \quad (68)$$

with

$$\alpha_n(E) = \left(n + \frac{1}{2}\right) + \left(\beta - \left(n + \frac{1}{2}\right)\right) \left(\frac{E}{E_{\text{asy}}}\right)^\gamma, \quad (69)$$

where $\beta < 0$, γ , and E_{asy} are nonlinear parameters. In the present case we have calculated the LIT up to 1000 MeV and thus we set $E_{\text{asy}} = 1000$ MeV, i.e. all basis functions have an asymptotic fall-off with E^β at $E = 1000$ MeV. The

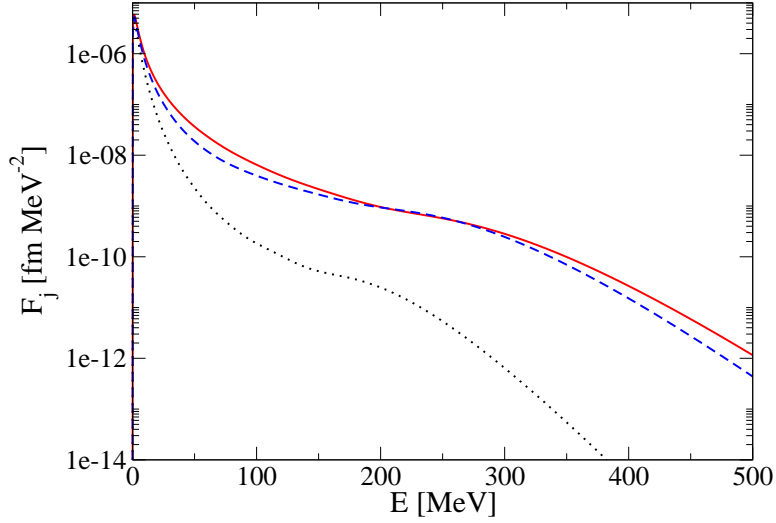


FIG. 5: (Color online) Strength function $F_j(E)$ for $j = 0$ (dotted), $j = 1$ (solid), $j = 2$ (dashed).

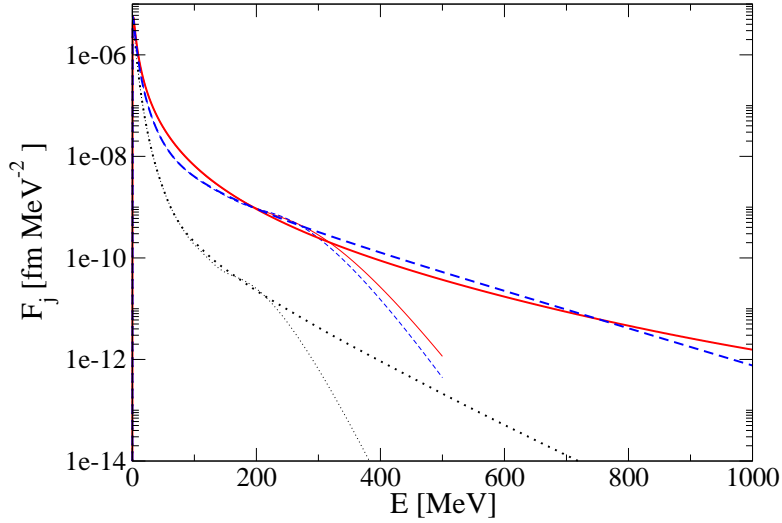


FIG. 6: (Color online) Strength functions F_j from inversions with first (thin lines) and second basis set (thick lines): $j = 0$ (dotted), $j = 1$ (solid), $j = 2$ (dashed).

inversions with basis set $\{\chi^{(2)}\}$ are shown in Fig. 6. At lower energies one finds a similar picture as in Fig. 5, the high-energy behavior, however, is quite different. One further notes that a constant asymptotic high-energy fall-off is already reached at energies considerably lower than $E_{\text{asy}} = 1000$ MeV showing that this set is a very good choice.

Figure 6 also shows that at lower energies the inversion results do not depend significantly on the choice of the basis set. On the other hand the precision of the agreement is difficult to judge on a logarithmic scale. Therefore, we show in Fig. 7 the various inversions at lower energies in a more detailed form, i.e. as relative differences

$$\Delta_j(E) = (F_j^{(1)}(E) - F_j^{(2)}(E))/F_j^{(2)}(E), \quad (70)$$

where $F_j^{(1)}$ and $F_j^{(2)}$ correspond to the inversions with the first and the second basis set, respectively. At very low energies one finds the largest differences for F_1 , namely about 7%. This relatively large difference is due to the steep rise of the strength function right above threshold. Here we would like to mention that, as suggested before, our first basis set leads to a better fit of the calculated LITs in the low σ_R region. Furthermore, Fig. 7 shows that up to 50 MeV further differences remain very small, in fact less than about 1%. For F_1 and F_2 the picture does not change very much for higher energies, whereas in case of F_0 the difference increases quite substantially beyond 80 MeV. This can be interpreted as a precursor effect for the strong fall-off beyond 200 MeV which leads to a somewhat oscillating inversion result already at considerably lower energies. In order to have the best description in the whole energy range

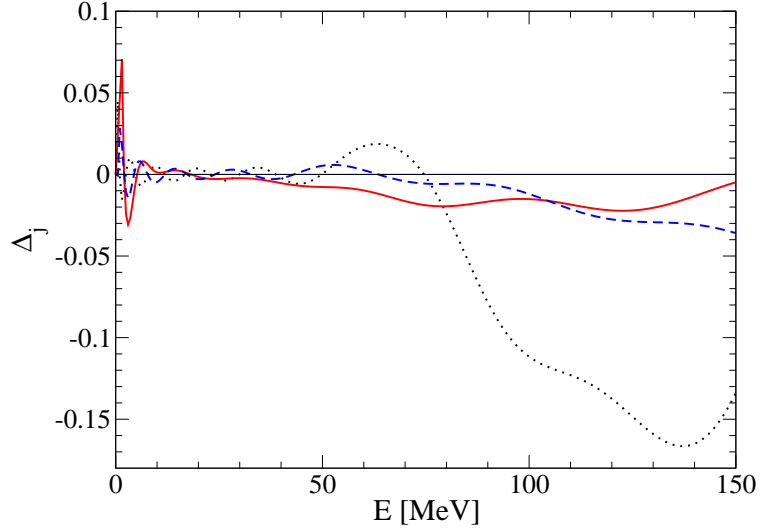


FIG. 7: (Color online) Relative differences $\Delta_j(E)$ of the strength functions shown in Fig. 6. Notation of curves as in Fig. 6.

we combine the inversion results of the two basis sets by taking $F_j^{(1)}(E)$ for $E \leq E_1$ and $F_j^{(2)}(E)$ for $E \geq E_1$ with E_1 equal to 30, 18, and 33 MeV for $j=0, 1, 2$, respectively.

The strength functions F_j can also be obtained from a standard calculation of deuteron photodisintegration. According to Ref. [1] one has

$$\text{Im } P_J(E1, E1) = 4\pi k \sum_j (-)^j \begin{Bmatrix} 1 & 1 & J \\ 1 & 1 & j \end{Bmatrix} \sum_{\mu ls} |E^1(\mu, jls)|^2, \quad (71)$$

where the $E1$ -matrix elements are defined by the multipole expansion of the total unpolarized photo absorption cross section [23, 24]

$$\sigma_0 = \frac{(4\pi)^2}{3} \sum_{L\mu, jls} \frac{1}{2L+1} (|E^L(\mu, jls)|^2 + |M^L(\mu, jls)|^2). \quad (72)$$

Here, the quantum numbers (μls) classify the various components of a two-body scattering solution with total angular momentum j [23, 24]. Comparison with Eq. (64) yields the relation

$$F_j(k + E_0) = \frac{8}{3k(2j+1)} \sum_{\mu ls} |E^1(\mu, jls)(k)|^2. \quad (73)$$

A comparison of the standard calculation with the LIT approach is shown in Fig. 8. The agreement is quite satisfactory in view of the fact, that in the standard calculation the complete $E1$ -operator is used and not its low energy form as in the present LIT approach.

Having obtained the reduced strength $F_j(E)$, one can then determine with the help of Eqs. (64) and (65) the imaginary and real parts of the polarizabilities $P_j^{\text{res}}(E1, E1, k)$. In Fig. 9 we compare our results for the polarizabilities to those of [1]. One should note that the real parts are normalized to zero at $k = 0$ for $J = 0$ and 2, which is not necessary for $J = 1$ since one has $P_j^{\text{res}}(E1, E1, k = 0) = 0$. This normalization takes into account implicitly the neglected contributions of the two-photon amplitude at $k = 0$, which are needed in order to comply with the low energy theorem of Eq. (32) for $J = 2$, whereas for the scalar polarizability we have to add the classical Thomson limit to the normalized resonance part according to

$$\text{Re}(P_0(E1, E1, k)) = \text{Re}(P_0^{\text{res}}(E1, E1, k)) - \frac{3e^2}{m_d}, \quad (74)$$

where m_d is the deuteron mass. This procedure is justified according to the discussion in [18] (see Fig. 3 of [18]), where it is shown that further contributions to the two-photon amplitude beyond the low energy limit are negligibly small for $k \leq 40$ MeV and remain quite small up to about 60 MeV. Thus, for calculations below 60 MeV, it seems to be quite safe to simply add the Thomson term to the normalized resonance $E1E1$ scalar polarizability.

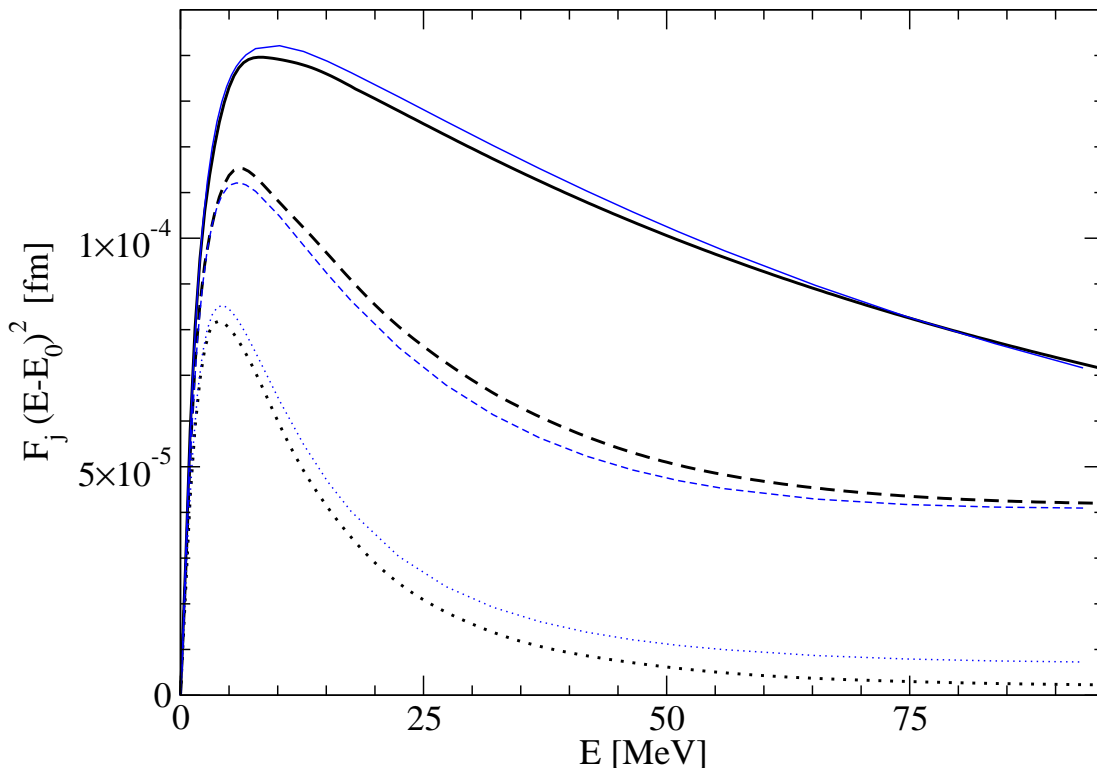


FIG. 8: (Color online) Strengths functions $F_j(E)$ weighted with $(E - E_0)^2$ for the Argonne V18 potential in standard approach with complete $E1$ -operator (thin lines) and LIT result with low energy $E1$ -operator (thick lines): $j = 0$ (dotted), $j = 1$ (solid), $j = 2$ (dashed).

With respect to the comparison in Fig. 9, we should mention that the polarizabilities of [1] are calculated in the Breit system. The relation between the photon momentum k of the Breit to that of the cm system depends on the scattering angle. Only in forward direction they turn out to be exactly the same. In addition it should be mentioned that in [1] a more complete calculation has been made where the full nuclear one-body current and also pion exchange currents have been taken into account. Furthermore, in [1] a different NN potential has been used. Despite these differences, one finds a rather good agreement between the two calculations for the scalar and tensor polarizabilities. Larger differences are found for the vector polarizability, for which real and imaginary parts from [1] are somewhat larger than our results. In Fig. 9 also the imaginary parts of the P_J evaluated by the standard method are shown. For $J = 0$ and 2 they are very similar to our results, actually the agreement is even better than one would expect from the results of Fig. 8. On the other hand, for $J = 1$ the standard result agrees quite well with that of Ref. [1]. However, one should keep in mind, that the vector polarizability is about an order of magnitude smaller than the scalar one due to large cancellations between the F_j . Thus the small differences in the F_j according to Fig. 8 result in considerably larger differences in P_1 .

With the calculated polarizabilities we can determine the cross section for pure E1 transitions given in (37). In Fig. 10 we show the resulting cross section in comparison to experimental data at $k_{\text{lab}} = 55$ MeV. One sees that our theoretical result overestimates slightly the experimental cross section, although within the experimental errors. Since data exist only for a very limited angular range one cannot draw any conclusion whether the E1E1 cross section reproduces the correct angular shape. However, from other theoretical calculations [1, 3–6] mentioned above, it is known that additional polarizabilities $P_j^{\text{res}}(M^{\nu'} L', M^{\nu} L, k)$ from neglected other multipoles, e.g. $M1$ and $E2$, play a considerably less important role at lower energies. Furthermore, in Refs. [3–6], it is pointed out that also the internal nucleon polarizabilities lead to non-negligible contributions. In fact, one aim of present-day Compton scattering experiments on light nuclei is the determination of the nucleon static electric and magnetic dipole polarizabilities, in particular the ones of the neutron.

We summarize our work as follows. After a brief overview over the theory of photon scattering, we have described as the central issue of our work the application of the LIT method to the calculation of the photon scattering amplitude. This method has the great advantage over conventional methods, since the resonance amplitude can be evaluated in a very efficient way, in which wave functions of the continuum spectrum of a particle system have not to be calculated

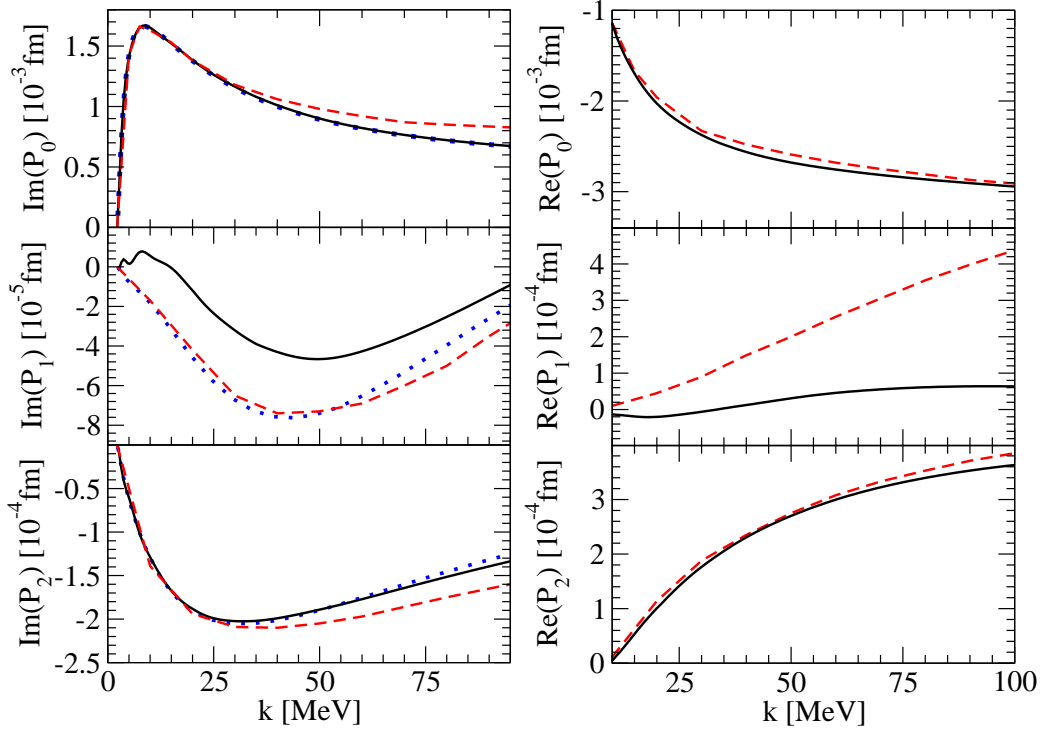


FIG. 9: (Color online) Imaginary (left panels) and real (right panels) parts of the polarizabilities $P_J^{\text{res}}(E1, E1, k)$ (solid) in comparison to those of [1] (dashed): $J = 0$ (top panels), $J = 1$ (middle panels), $J = 2$ (bottom panels). Note that the real parts are normalized to zero at $k = 0$ (see text). For the imaginary parts also the results with from the standard calculation are shown (dotted)

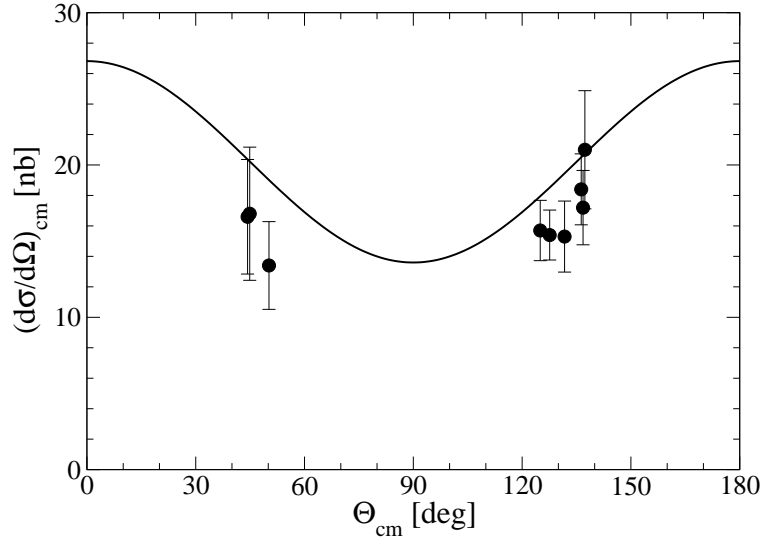


FIG. 10: Comparison of the differential scattering cross section in the unretarded dipole approximation with experimental data from [25] ($k_{\text{lab}} = 55$ MeV).

explicitly. Because of this reason, and in contrast to conventional state-of-the-art methods, the LIT approach can be applied also to systems with more than three particles.

As a first application and test case, we have considered elastic photon scattering off the deuteron at low energies. For this case we have taken into account only E1 transitions in the unretarded dipole approximation. In order to apply the LIT method one has to invert the calculated integral transforms of the so-called strength functions. This inversion is discussed in great detail. In particular the high-energy behavior of the strength functions is studied with great

care. We have compared the resulting three E1E1 polarizabilities with results from conventional calculations. The comparison has shown the reliability of the obtained results. At last we have confronted the E1E1 cross section with experimental data at a photon energy of 55 MeV. In view of the approximations of the present work the agreement is quite satisfactory. This is certainly a strong encouragement to consider in future work photon scattering off more complex light nuclei.

-
- [1] M. Weyrauch and H. Arenhövel, Nucl. Phys. A **408**, 425 (1983).
 - [2] M.I. Levchuck, Few Body Syst., Suppl. **9**, 439 (1995).
 - [3] J.J. Karakowski and G.A. Miller, Phys. Rev. C **60**, 014001 (1999).
 - [4] M.I. Levchuck and A.I. L'vov, Nucl. Phys. A **674**, 449 (2000); Nucl. Phys. A **684**, 490 (2001).
 - [5] R.P. Hildebrandt, H.W. Griefhammer, T.R. Hemmert, and D.R. Phillips, Nucl.Phys. A **748**, 573 (2005).
 - [6] R.P. Hildebrandt, H.W. Griefhammer, and T.R. Hemmert, Eur. Phys. J. A **46**, 111 (2010).
 - [7] G. Feldman, priv. comm.
 - [8] V.D. Efros, W. Leidemann and G. Orlandini, Phys. Lett. B **338**, 130 (1994).
 - [9] V.D. Efros, W. Leidemann, G. Orlandini, and N. Barnea, J. Phys. G: Nucl. Phys. **34**, R459 (2007).
 - [10] S. Bacca, M.A. Marchisio, N. Barnea, W. Leidemann, and G. Orlandini, Phys. Rev. Lett. **89**, 052502 (2002).
 - [11] S. Bacca, H. Arenhövel, N. Barnea, W. Leidemann, and G. Orlandini, Phys. Rev. C **76**, 014003 (2007).
 - [12] H. Arenhövel, *New Vistas in Electro-Nuclear Physics*, eds. E.L. Tomusiak, H.S. Caplan, E.T. Dressler (Plenum Press, New York 1986) p. 251.
 - [13] J.L. Friar, Ann. Phys. (N.Y.) **95**, 1428 (1975).
 - [14] H. Arenhövel and M. Weyrauch, Nucl. Phys. A **457**, 573 (1986).
 - [15] M.E. Rose, *Elementary theory of angular momentum*, (Wiley, New York, 1957).
 - [16] A.R. Edmonds, *Angular momentum in quantum mechanics*, (Princeton University Press, Princeton, 1957).
 - [17] H. Arenhövel and W. Greiner, Prog. Nucl. Phys. Vol. **10** (1969) 167 (Pergamon Press, Oxford).
 - [18] M. Weyrauch, Phys. Rev. C **38**, 611 (1988).
 - [19] R.B. Wiringa, V.G.J. Stoks and R. Schiavilla, Phys. Rev. C **51**, 38 (1995).
 - [20] V.D. Efros, W. Leidemann, G. Orlandini, and E.L. Tomusiak, Phys. Rev. C **81**, 034001 (2010).
 - [21] D. Andreasi, W. Leidemann, Ch. Reiß and M. Schwamb, Eur. Phys. J. A **24**, 361 (2005).
 - [22] N. Barnea, V.D. Efros, W. Leidemann and G. Orlandini, Few-Body Syst. **47**, 201 (2010).
 - [23] F. Partovi, Ann. Phys. (N.Y.) **27**, 79 (1964).
 - [24] H. Arenhövel and M. Sanzone, Few-Body Syst. Suppl. **3**, 1 (1991).
 - [25] M. Lundin et al., Phys. Rev. Lett. **90**, 192501 (2003).